

REAL-TIME NATION-WIDE PRODUCTION OF 3D WIND AND REFLECTIVITY FIELDS IN FRANCE: SCIENCE, ENGINEERING AND APPLICATIONS

Antoine Kergomard*, Pascale Dupuy, Pierre Tabary and Olivier Bousquet
Centre de Météorologie Radar, Météo-France, Toulouse, France

1. Introduction

From November 2006 to September 2008, real-time analysis of multiple-Doppler data collected by the French operational radar network have been performed and evaluated over the greater Paris area using the well-established MUSCAT (multiple-Doppler synthesis and continuity adjustment technique) algorithm initially proposed by Bousquet and Chong (1998). Since the results of this experiment were convincing (Bousquet 2008), it has been envisaged to extend the retrieval domain to the whole of France, using the 24 French radars.

This paper presents the different experiments that were conducted in order to validate the real-time reflectivity and wind products over such a large area. Different sensitivity tests to the interpolation parameters and to the compositing algorithms were carried. Given high-resolution 3D reflectivity and wind fields as a reference, the reflectivity and radial velocity PPIs of all radars were simulated, taking into account the operational scanning strategy. Comparing the retrieved field to the reference enabled to assess the efficiency of the retrieval and to optimize the parameters used in the retrieval algorithm. In order to limit the computing time, the national domain has been divided into 4 overlapping sub-domains.

The final product, available in real-time every 15 minutes with a horizontal resolution of 2.5 km and a vertical resolution of 500 m, is a 3D grid giving the interpolated reflectivity, wind field (u , v and w) and divergence values, all together with some quality indicator.

An experimentation is currently being held with the forecasters to assess the benefit of the product in monitoring the realism of the wind structures depicted by the mesoscale numerical model (AROME).

2. The French radar network

The French operational weather radar network, named ARAMIS (Application Radar a la Météorologie Infra-Synoptique), was initially built for rain detection purposes. In 2002, an upgrade program, called Programme Aramis Nouvelles Technologies en Hydrométéorologie Extension et Renouvellement (PANTHERE), was initiated in partnership with the French Ministry of Environment to complete and extend this network (Parent et al. 2003) and implement Doppler and dual-polarimetry capabilities. As of today, 7 new Doppler radars have been installed, 2 have been replaced, and a numerical

receiver has been developed to dopplerize the older radars.

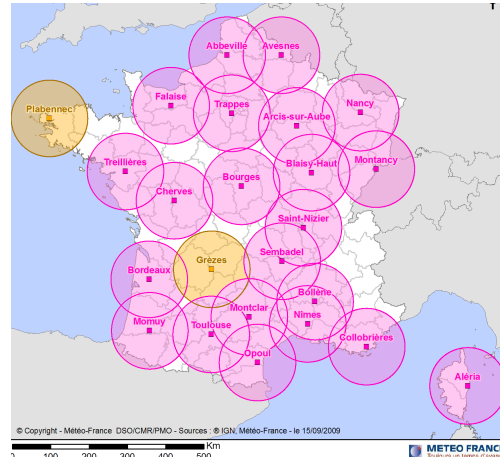


Figure 1: Map of the French radar network as of August 2009. Circles show the 100 km range of measurement. Colors indicate the kind of radars (Doppler or not)

The network comprises 22 Doppler radars (Figure 1) covering about 95 % of the French territory with radar baselines ranging from ~180 km in the northern part of the country down to less than 60 km in the south east of France. The triple-PRT scheme proposed by Tabary et al. (2006) is operationally deployed. It is being revised (Augros, 2009) in order to decrease the number of spurious echoes and to limit the rate of aliased velocities, keeping the useful range up to 250 km.

3. Current configuration of real time 3D chain

All radars perform a complete volume scan in 15 minutes (a supercycle) according to the operational modes showed in Table 1. The current scanning strategy consists in 3 to 5 elevation angles every 5 minutes and is radar specific.

Input data are operational PPIs of Doppler velocity and reflectivity projected on a 1 km^2 Cartesian grid (same data as for assimilation into the mesoscale model AROME). They are synchronized with respect to the ending time of the current 15' supercycle to account for the non-simultaneity of measurements. Spurious reflectivity and radial velocity data are removed using a threshold on the pulse-to-pulse fluctuation of the reflectivity and a $5 \times 5 \text{ km}^2$ median filter, respectively.

*Corresponding author address: antoine.kergomard@meteo.fr

| | PPI | | | | | | | | | | | | | | | | | |
|--------------|-----|-----|-----|-----|-----|-----|-------------------------|-----|-----|-----|-----|-----|-------------------------|-----|-----|-----|-----|-----|
| | 1 | 2 | 3 | 4 | 5 | 6 | 7 | 8 | 9 | 10 | 11 | 12 | 13 | 14 | 15 | 16 | 17 | 18 |
| Abbeville | 0,4 | 1,1 | 0,4 | | | | Previous cycle repeated | | | | | | Previous cycle repeated | | | | | |
| Arcis | 4 | 1,1 | 0,4 | | | | 3 | 1,1 | 0,4 | | | | 2 | 1,1 | 0,4 | | | |
| Avesnes | 90 | 7 | 4 | 1,6 | 1 | 0,4 | 9 | 6 | 3 | 1,6 | 1 | 0,4 | 8 | 5 | 2 | 1,6 | 1 | 0,4 |
| Blaisy | 3,6 | 2,6 | 1,6 | 1 | 0,5 | | Previous cycle repeated | | | | | | Previous cycle repeated | | | | | |
| Bollene | 6 | 2,4 | 1,8 | 1,2 | 0,8 | 0,4 | 4,8 | 2,4 | 1,8 | 1,2 | 0,8 | 0,4 | 3,6 | 2,4 | 1,8 | 1,2 | 0,8 | 0,4 |
| Bordeaux | 9 | 1,5 | 0,4 | | | | Previous cycle repeated | | | | | | Previous cycle repeated | | | | | |
| Bourges | 3,2 | 2,2 | 1,3 | 0,7 | | | 4,2 | 2,2 | 1,3 | 0,7 | | | 5,2 | 2,2 | 1,3 | 0,7 | | |
| Cherves | 0,4 | 2,6 | 1,6 | 1 | 0,4 | | 0,4 | 3,6 | 1,6 | 1 | 0,4 | | 0,4 | 4,6 | 1,6 | 1 | 0,4 | |
| Collobrieres | 4,8 | 3,6 | 2,2 | 1,4 | 0,4 | 0,8 | 6 | 3,6 | 2,2 | 1,4 | 0,4 | 0,8 | 7,2 | 3,6 | 2,2 | 1,4 | 0,4 | 0,8 |
| Falaise | 1,6 | 1,1 | 0,4 | | | | Previous cycle repeated | | | | | | Previous cycle repeated | | | | | |
| Grezes | 2,6 | 1,6 | 1 | 0,4 | | | Previous cycle repeated | | | | | | Previous cycle repeated | | | | | |
| Momuy | 90 | 5,6 | 2,6 | 1,6 | 1 | 0,4 | 7,6 | 4,6 | 2,6 | 1,6 | 1 | 0,4 | 6,6 | 3,6 | 2,6 | 1,6 | 1 | 0,4 |
| Montancy | 90 | 5 | 2,2 | 1,2 | 0,7 | 0,4 | 7 | 3,9 | 2,2 | 1,2 | 0,7 | 0,4 | 6 | 3 | 2,2 | 1,2 | 0,7 | 0,4 |
| Montclar | 90 | 5,5 | 2,5 | 1,6 | 1 | 0,4 | 7,5 | 4,5 | 2,5 | 1,6 | 1 | 0,4 | 6,5 | 3,5 | 2,5 | 1,6 | 1 | 0,4 |
| Nancy | 2,5 | 1,9 | 1,3 | 0,7 | | | Previous cycle repeated | | | | | | Previous cycle repeated | | | | | |
| Nimes | 8 | 3,5 | 2,4 | 1,8 | 1,2 | 0,6 | 9,5 | 5 | 2,4 | 1,8 | 1,2 | 0,6 | 90 | 6,5 | 2,4 | 1,8 | 1,2 | 0,6 |
| Opoul | 3 | 1,4 | 1 | 0,6 | | | Previous cycle repeated | | | | | | Previous cycle repeated | | | | | |
| Plabennec | 3 | 2 | 0,8 | 0,4 | | | Previous cycle repeated | | | | | | Previous cycle repeated | | | | | |
| Sembadel | 4 | 1,2 | 0,8 | 0,4 | | | 3 | 1,2 | 0,8 | 0,4 | | | 2 | 1,2 | 0,8 | 0,4 | | |
| StNizier | 4 | 1,6 | 1 | 0,4 | | | 3 | 1,6 | 1 | 0,4 | | | 2,2 | 1,6 | 1 | 0,4 | | |
| Toulouse | 90 | 8,5 | 5,5 | 2,5 | 1,5 | 0,8 | 10,5 | 7,5 | 4,5 | 2,5 | 1,5 | 0,8 | 9,5 | 6,5 | 3,5 | 2,5 | 1,5 | 0,8 |
| Trappes | 90 | 7,5 | 0,8 | 1,5 | 4,5 | 0,4 | 9,5 | 6,5 | 0,8 | 1,5 | 3,5 | 0,4 | 8,5 | 5,5 | 0,8 | 1,5 | 2,5 | 0,4 |
| Treillieres | 2,1 | 1,5 | 0,8 | 0,4 | | | 3 | 1,5 | 0,8 | 0,4 | | | 4 | 1,5 | 0,8 | 0,4 | | |

Table 1: scanning strategy of the 23 radars covering the France. A super cycle (18 tilts) is composed of three 5' cycles (6 tilts).

Once pre-processed, data are interpolated into the retrieval Cartesian grid using a fixed horizontal influence radius of the Cressman weighting function R_H of 3 km and a variable vertical radius of influence R_V equal to 1° (beamwidth of the ARAMIS radars). In this configuration, R_V varies as a function of range so that the search for data points extends farther out at long range compared to short range. At long range, this also allows to indirectly take into account the lost of resolution resulting from beam broadening. Once interpolated, data are ingested in the MUSCAT analysis (Bousquet and Chong 1998; Chong and Bousquet 2001).

The national retrieval domain is a Cartesian domain measuring 1000 km x 1100 km x 12 km, covering the whole country (except Corsica). The vertical resolution is set to 500 m. The horizontal resolution is set to 2.5 km to be consistent with unavoidable smoothing inherent to radar beamwidths and baselines of $\sim 1^\circ$ and ~ 180 km, respectively.

With simulated PPIs corresponding to the different elevations used operationally for each radar (see Table1), it is possible to calculate the wind and reflectivity coverage. The interpolation parameters used for the simulation are those described before ($R_H=3km$, R_V equal to 1° ; minimum number of data inside the Cressman ellipsoid set to 5). The best coverage is encountered between the altitudes of

3000 and 6000 m (Figure 2). At 1000 m, the coverage is quite poor. In practice, it is even poorer due to orography, which is not taken into account in the simulation.

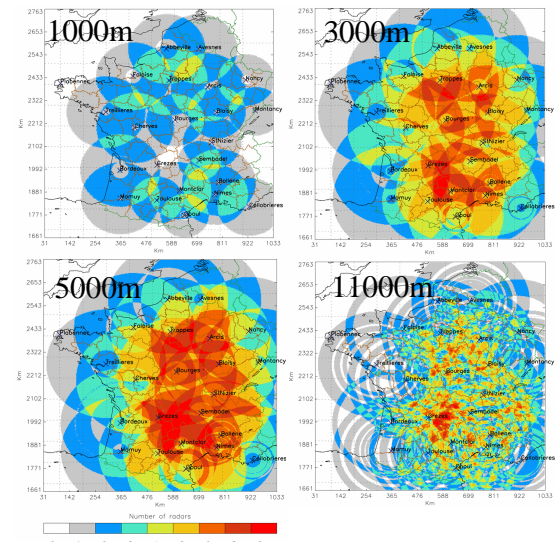


Figure 2: Doppler radar overlapping at various heights within the national domain shown in Fig. 1

To challenge the computing time, the national domain is divided into 4 overlapping domains, measuring 510 km x 562 km x 12 km, as shown in Figure 3. Working with 4 sub-domains, on a 4 processors machine, divides the computing time up to 4, in the case of widespread precipitations. A linear interpolation is used to obtain wind and reflectivity fields at the junction areas. Thus, the final product is ready at worst 15 minutes after all input data are available, instead of up to 1 hour with only one big domain.

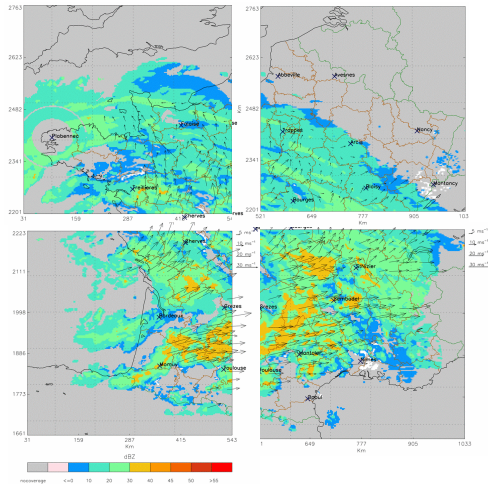


Figure 3. Reflectivity and wind-field for each retrieval sub-domain, on 24 January at 03:30, at level 2000m.

4. Testing the algorithm performances and defining a quality flag

It has been chosen to use horizontally uniform reference fields, vertically defined as follow. Reflectivity vertically decreases from 50 dBZ at a rate of -3dB/km until 10km, at a rate of -12dB/km above. Wind rotates with altitude. The two horizontal components are given by:

$$u = 20 \sin\left(\frac{\pi z}{2 z_0}\right) \quad v = 20 \cos\left(\frac{\pi z}{2 z_0}\right) \quad z_0 = 3000m$$

There is no vertical component.

PPIs have been simulated from these reference fields in accordance with the operational scanning strategy, and next used as input of the 3D retrieval algorithm on the national domain.

The first reflectivity composites have been obtained using the maximum reflectivity algorithm, defined as follow:

$$Z_{\text{pixel}}(\text{mosaic}) = \max_{\text{radar}}(Z_{\text{pixel}}(\text{radar}))$$

It has been then noted that the reflectivity retrieved field was overestimated at high altitudes, because of the influence of the increasing with range vertical Cressman radius. Decreasing this radius (to 0.5°) leads to lessen the coverage; furthermore, the quality of the final product is degraded, due to the decrease of the number of radar data available.

The following algorithm has finally been chosen, that takes into account the distance from the contributing radars:

$$\omega_{\text{radar}} = \exp\left(-\frac{d_{\text{radar-pixel}}^2}{R_{\text{max}}^2}\right) \quad \text{with } R_{\text{max}} = 50$$

Figure 4 shows a vertical latitudinal retrieved reflectivity cross-section over France compared with the reference field. The retrieved field is in line with the reference up to 10 km.

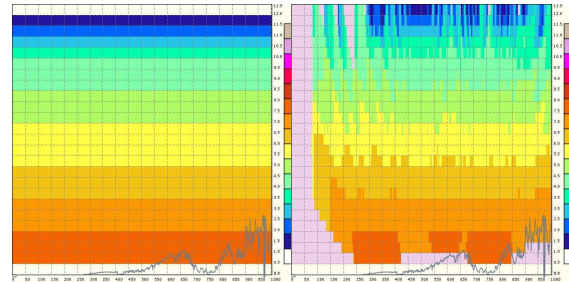


Figure 4 : Latitudinal Vertical cross-section of reflectivity (left reference, right retrieved)

A quality flag has been defined, which takes into account the distance between one pixel and the radars contributing to this pixel. For each pixel and for each radar, the following parameter is computed, and then composited with the same method as for reflectivity:

$$\Delta Z = \Delta Z_0 + a \cdot \frac{d}{d_0}$$

$$\text{with } \Delta Z_0 = 3\text{dBZ}, a = 3 \text{ and } d_0 = 250\text{km}$$

The comparison between the retrieved and the reference reflectivity field shows that this quality flag seems to slightly overestimate the uncertainty, but is correctly spatially distributed.

Figure 5 shows the same vertical cross-section as above for the norm of the latitudinal component of the wind.

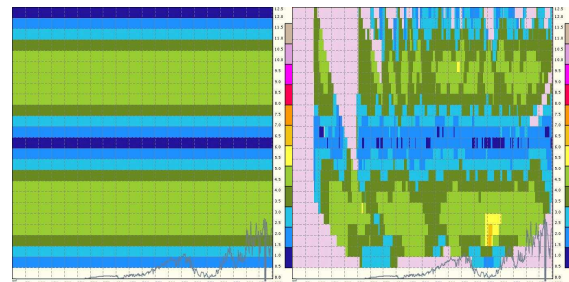


Figure 5 : Latitudinal Vertical cross-section of wind (left reference, right retrieved)

The wind field is correctly retrieved, with no major shift along the vertical.

It is foreseen to develop a quality indicator for wind, with the same idea than for reflectivity, giving a kind of uncertainty of the retrieved value.

5. Examples of 3D wind and reflectivity real time retrievals

5.1 Klaus storm

This paragraph presents some results from the 3D real-time retrieval algorithm. The first example is the severe storm Klaus which hit France on 24th January 2009.

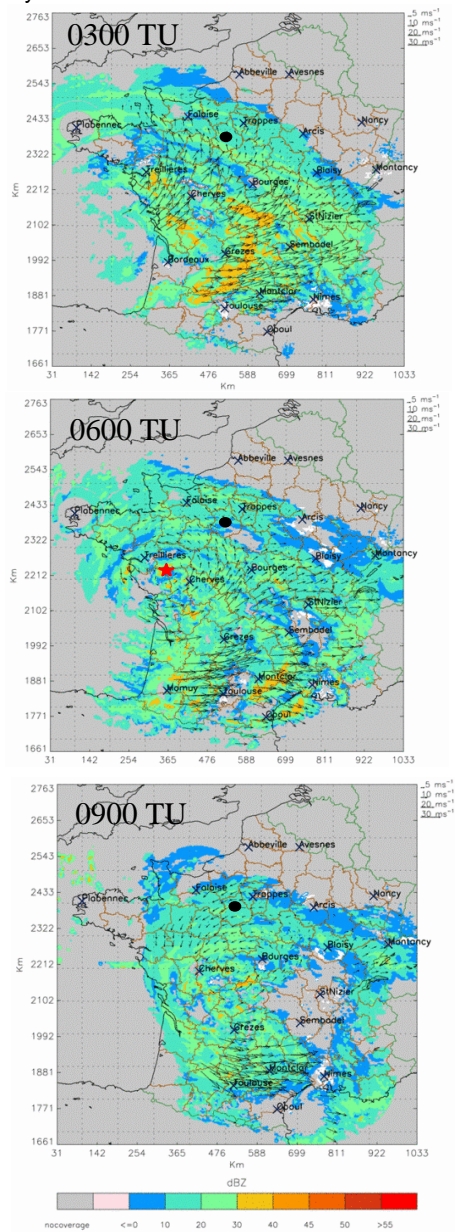


Figure 6: reflectivity and wind at 2000m, at 03, 06 and 09 UTC during Klaus storm, on 24th January 2009. The red star is the location of the low-pressure area center at 2000m analyzed by ALADIN model. The black point locates La Ferté Vidame wind-profiler.

As shown in Figure 6, the location of the center of the low analyzed by the ALADIN model (red cross) is in good agreement with the retrieved wind field.

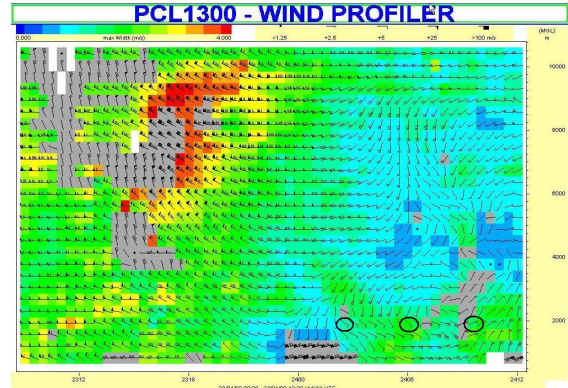


Figure 7: La Ferté-Vidame wind-profiler data, during Klaus storm

The only other altitude observations available during the Klaus storm are the data from the wind-profiler in La Ferté Vidame, which is located 70km southwest of Paris. Although this wind-profiler is north of the maximum wind area, the comparison with the 3D retrieved wind shows a good agreement (Figure 7). At 0300 and 0600 UTC, the wind at an altitude of 2000m is south and around $5\text{m}\cdot\text{s}^{-1}$. At 0900TU, both the 3D wind and the wind measured by the profiler have turned east, and strengthened.

5.2 Hail event

The 3D retrieved reflectivity allows computing a derivate probability of hail, using the following formula (Delobbe and Holleman, 2006):

$$POH=0.319+0.133\times(Alt_{iso-45dBZ}-Alt_{iso0^{\circ}C})$$

The iso-0°C altitude is taken from ALADIN model analysis.

Figure 8 shows the POH calculated every 15 minutes on the 15 May 2008 from 1700 (black) to 2030 UTC (orange). The red crosses represent the hailpads where hailstones (with diameters greater than 5 mm) were observed, the white crosses the hailpads where no hail was reported. The trajectories of the two cells that gave hail are well detected by the radar. The number of false alarms from the radar is rather high. Some studies are at the present conducted to optimize the hail detection, taking advantage of the dual polarization when available (Tabary, 2009).

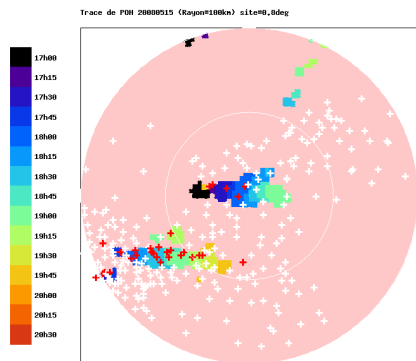


Figure 8: hail imprints on the 1(May 2008. The crosses are the hailpads, in red when hail was reported

6. Conclusions

It has been demonstrated that running a real time 3D chain was feasible over the whole of France, with a computing time of 10 to 15 minutes. The results were validated using simulated data and on some severe weathers cases. The product is now being evaluated in real time by the forecasters.

Many improvements are expected by next year. The wind retrieval coverage should increase with the radars of Plabennec and Grezes being dopplerized in 2010. Quality flags will be added to wind parameters. Changes in the projection of the retrieval grid (not to re-project as now from Lambert 2 initial projection to Polar Stereographic projection) will permit to gain time. By computing the reflectivity field first apart from the wind, it should be possible to have the reflectivity mosaic available much sooner as it is now. Tests have already been done, and show that the reflectivity mosaic could be available at H+5, instead of H+10 to H+15 in the current real-time chain. Taking orography into account is another way to improve the current interpolation algorithm.

To complete the current product and in order to synthesize the 3D information, it is foreseen to add 2D fields such as VIL (vertically integrated liquid content), Zmax, altitude of Zmax, EchoTop, with a higher resolution (1 km²) and a frequency of 5 minutes. Those products will be used as an input for nowcasting applications. Those products will be computed by advecting and extrapolating the 3D

product on a 1 km² resolution grid, and applying the obtained VPR to the 2D reflectivity high resolution image (Le Henaff, 2007)

References

- Augros C, Tabary P, 2009: Improvements of the French operational triple-PRT Doppler scheme, 34th Radar Conference, 5-9 october, Williamsburg, VA, USA
- Delobbe, L., and I. Holleman, 2006 : Uncertainties in radar echo top heights used for hail detection, /Meteorol. Appl./, *13*, 361 – 374.
- Bousquet O., and M. Chong, 1998: A multiple Doppler and continuity adjustment technique (MUSCAT) to recover wind components from Doppler radar measurements. J. Atmos. Oceanic Technol., **15**, 343-359.
- Bousquet O., P. Tabary, and J. Parent du Châtelet, 2007: On the value of operationally synthesized multiple-Doppler wind fields. Geophys. Res. Letter, Accepted pending minor revisions.
- Browning K., A., and R. Wexler, 1968: The determination of kinematic properties of a wind field using Doppler radar, *J. Appl. Meteorol.*, **7**, 105–113
- Chong, M., and O. Bousquet, 2001: On the application of Muscat to a ground-based dual-Doppler radar system. Meteorol. Atmos. Phys., **78**, 133-139
- Doviak and Zrnica, 1993: Doppler radar and weather observations (second edition), Academic Press, Inc.
- Parent-du-Châtelet, J., M. Guimera, and P. Tabary, 2003: The PANTHERE Project of Meteo-France: Extension and upgrade of the French radar network. Preprints, *31st Int. Conf. on Radar Meteorology*, Seattle, WA, Amer. Meteor. Soc., 802–804.
- Tabary, P., F. Guibert, L. Perier, and J. Parent-du-châtelet, 2006: An operational triple-PRT scheme for the French radar network. J. Atmos. Oceanic Technol., **23**, 1645-1656.
- Bousquet O., Tabary P and Parent du Châtelet J., 2007, Operationnal Multiple Doppler Wind Retrieval Inferred from Lon-Range Radial Velocity Measurement, Journal Of Applied Meteorology and Climatology 47.
- Le Henaff A., 2007, Produit radar multi-couches pour DPREVI/PI dans le cadre de FLYSAFE, internal document, Météo France
- Tabary P., Fradon B., Dupuy P., Ilingworth J. and Vulpiani G., Hail detection and quantification with a C-band polarimetric radar : Challenge and promises, 34th Radar Conference, 5-9 october, Williamsburg, VA, USA